Mechanically versatile isosorbide-based thermoplastic copolyether-esters with a poly(ethylene glycol) soft segment

Peer-reviewed author version

MONNERY, Bryn; KARANASTASIS, Apostolos; ADRIAENSENS, Peter & PITET, Louis (2021) Mechanically versatile isosorbide-based thermoplastic copolyether-esters with a poly(ethylene glycol) soft segment. In: Journal of Polymer Science, 59(22), p. 2809-2818.

DOI: 10.1002/pol.20210548
Handle: http://hdl.handle.net/1942/35499

Mechanically versatile isosorbide-based thermoplastic copolyether-esters with a poly(ethylene glycol) soft segment

Bryn D. Monnery[†], Apostolos Karanastasis[†], Peter Adriaensens[‡], Louis M. Pitet[†*]

[†]*Advanced Functional Polymers Group,* [‡]*Applied and Analytical Chemistry Group*, [†‡]*Institute for Materials Research (IMO), Hasselt University, Martelarenlaan 42, 3500 Hasselt, Belgium.*

ABSTRACT

Segmented thermoplastic copolyether esters (TPEEs) with a partially renewable hard block containing isosorbide (ISB) and poly(ethylene glycol) (PEG) soft blocks were prepared by melt polycondensation. A range of compositions were accessible despite the relatively low reactivity of the sterically and electronically hindered ISB monomer. The small scale reactions performed in the melt were limited in terms of achievable molar mass. This is attributed to the challenge of attaining stoichiometric balance in the feed and maintaining this balance throughout the high temperature (>200 °C) reactions. Nevertheless, products were isolated that could be manipulated and melt-pressed into specimen for tensile testing. Varying the feed compositions gave rise to copolymers exhibiting a broad range of mechanical properties (elastic modulus from 1 MPa – 66 MPa). These characteristics are consistent with a segmented polymer architecture with morphological features similar to commercially available TPEE counterparts. These results pave the way for more responsibly sourced building blocks being incorporated into materials with high market value potential.

INTRODUCTION

Segmented thermoplastic copolyether esters (TPEEs) are an industrially important class of materials with an extremely wide application range.[1-4] They are commonly found in high performance areas, owing to the typical durability, thermo oxidative stability, and highly tunable mechanical profile.[5] This is an area ripe for further interrogation, and developments into efficient production and sustainable improvements in manufacturing are on-going.[6] TPEEs typically consist of multiple segments (i.e. blocks), with one type being a relatively rigid or hard segment (i.e., high T_g/T_m) and the other a flexible or soft segment (i.e., low T_g) (Figure 1a). Employing immiscible blocks give rise to microphase separated morphologies, with phases enriched in the either of the two segment types (Figure 1b). The hard segment conventionally consists of a semiaromatic, semi-crystalline polyester such as polybutylene terephthalate (PBT). Various soft segments have been employed, including poly(ethylene glycol) (PEG) of varying molar mass. Mechanical properties are tailored in a straightforward manner by adjusting the composition of the feed and through judicious selection of soft-block molar mass.[7] In this manner, a wide range of mechanical characteristics can be accessed, ranging from high modulus, rigid engineering thermoplastics at high hard-block content (φ_{HB} 10–30%) to low modulus, highly extensible elastomeric materials at low hard-block content (φ_{HB} 50–70%).

Despite the versatility afforded by the wide range of building blocks and compositions available for the preparation of TPEEs, nearly all commercially available variants are produced from fossil-based feedstocks. Furthermore, the hard segments are nearly always semi-crystalline and the processing windows are bound by the crystallization kinetics, which can vary dramatically with composition and corresponding hard block segment length. We sought to investigate the possibilities of preparing TPEEs that are fully amorphous and also based partially on renewable, biobased monomers, particularly for the hard segments.

The field of sustainable polymers from renewable monomers is a rapidly maturing area, with the spotlight on improving the plight of plastic waste that persists in the environment.[8-12] There have already been significant efforts to incorporate various bio-based/renewable building blocks into engineering polyesters via polycondensation processes in an effort to manipulate the properties and improve the impact in the context of sustainability.[13-16] Several diols derived from various sugars have been employed as substitutes for 1,4-butanediol or ethylene glycol in the engineering polyesters PBT and PET respectively.[14, 17, 18] Such examples include mannitol,[19-23] isosorbide,[24-28] isoidide[29-32] and others.[33-37]

In particular, isosorbide (ISB) has some appealing properties when combined in copolyesters.[29-31, 38-40] The most prominent examples have focused on combining ISB with terephthalate derivatives and other comonomers in order to generate statistical copolyesters. The polyester comprising isosorbide-terephthalate (ISB-T) repeat units is amorphous with a relatively high T_g (> 200 °C).[41-43] It can be challenging to synthesize based on the internal hydrogen bonding and relatively hindered sterics surrounding the hydroxyl groups. Nevertheless, reactivity has been promoted under several conditions to afford copolyesters.[44-47] To our knowledge, there are very few examples describing any soft blocks combined with ISB-T as hard segments in TPEEs. It is surmised that this absence of examples owes itself to the difficulty of reacting ISB with acids and esters, and the conventional two-stage protocol employed in the commercial manufacturing of TPEEs (*vide infra*). We feel that if this class of material could be accessed, many interesting new polymers could be uncovered.

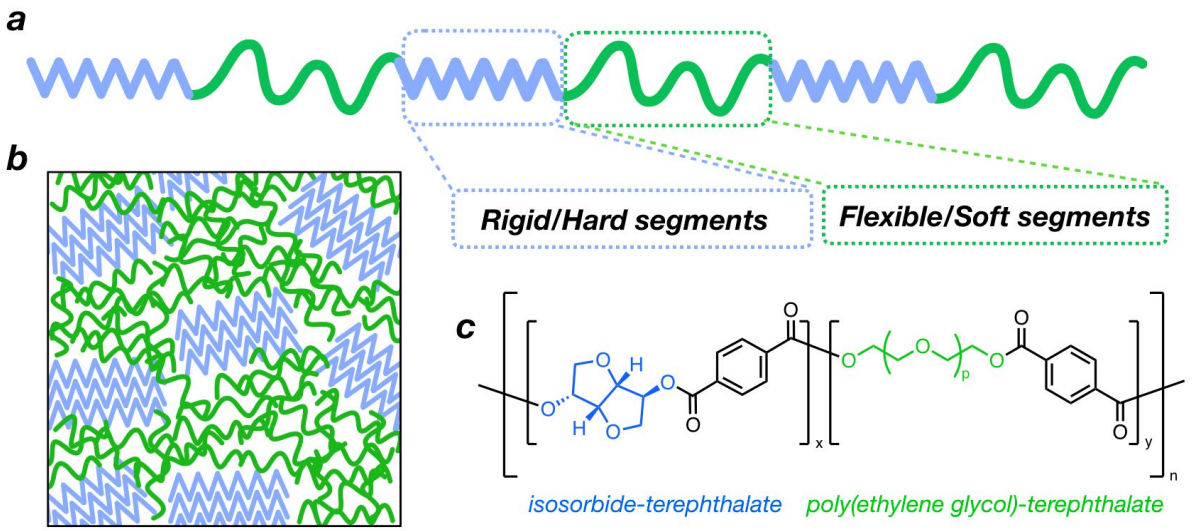

Figure 1. a) Illustration of segmented TPEEs with alternating rigid/hard blocks and flexible/soft blocks; b) illustration of typical morphology in a conventional segmented TPEE showing domain rich in soft block (green) physically crosslinked by domain rich in hard block (blue); c) chemical structure of a segmented multi-block copolymer consisting of hard ISB-T segments and soft PEG-T segments.

Here we investigate a particular class of segmented TPEE with PEG soft blocks and ISB-T hard blocks (Figure 1c). PEG in TPEEs is exploited for use in high-end fabrics like medical gowns, footwear, food packaging and outdoor sport clothing. The PEO provides exceptional permeation properties for breathability, while the segmented architecture and the hard component provide strength and durability. We aim to evaluate the possibility of replacing the hard PBT segments in conventional materials with a biobased, amorphous, high T_g alternative, derived from the transesterification of ISB and a terephthalate derivative.

Isosorbide was copolymerized with dimethyl terephthalate (DMT) and a PEG soft segment having a molar mass of 1000 g mol^{-1}, ultimately covering a range of compositions by adjusting the feed ratios (Scheme 1). The final multiblock segmented architecture was corroborated by ^{1}H and ^{13}C nuclear magnetic resonance (NMR) spectroscopy and relative molar masses were measured with size-exclusion chromatography (SEC). The thermal properties have been analyzed by differential scanning calorimetry (DSC) and are consistent with the structural characteristics elucidated by spectroscopic analysis. Finally, the tensile properties were assessed for melt-pressed samples.

Scheme 1. Polycondensation copolymerization involving DMT, ISB and PEG (M_n = 1000 g mol^{-1}) leading to a segmented TPEE.

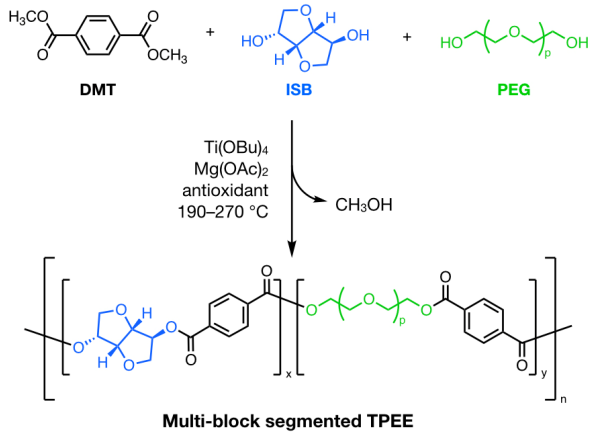

RESULTS AND DISCUSSION

The synthesis of these segmented TPEEs presents several conceptual and practical challenges. The conventional melt polycondensation employed to prepare PBT, PET and TPEEs involves the strategy of dosing excess volatile diol, namely 1,4-butane diol (BDO) or ethylene glycol (EG) for PBT and PET, respectively. The excess diol serves to promote extensive transesterification in an initial step that leads to oligomerization. If DMT is used as the terephthalate derivative, this first stage produces methanol as condensate, which is easily removed at elevated temperature (150–180 °C). The excess diol also provides a highly mobile melt phase that is easily mixed. Most importantly, the diols that are employed are relatively volatile at further elevated temperature (> 220 °C) and reduced pressure. Further transesterification and polycondensation causes expulsion of the diol and drives the equilibrium reaction towards stoichiometric balance. Viscosity rises rapidly during this stage as molar mass increases. The primary challenge in Scheme 1 involves the absence of a

volatile diol, or any component that could be removed by evaporation for that matter. Thus, the ability to reach reasonably high molar mass relies on the balance of complementary end-groups (i.e., hydroxyls and methyl esters) in the feed. The difficulty in doing so is exacerbated by the inclusion of a polymeric macromonomer (i.e., PEG) that has its own molar mass distribution. Therefore, there is inherent uncertainty associated with the end-group concentration contributed from the PEG component. The M_n of the PEG used in this study was determined with ^{1}H NMR spectroscopy. Despite this measurement based on end-group analysis being reasonably accurate, the associated uncertainty is nevertheless around 5%. Polycondensations are well-known to be highly sensitive to stoichiometric imbalance in terms of achievable molar mass. These factors make it a challenge not only to reach high molar mass, but also with consistency from batch to batch. Nevertheless, we have shown that samples with molar mass high enough to be mechanically robust can routinely be made, using a strictly executed synthetic protocol.

Copolymers were prepared by mixing the three co-monomers in various ratios, carefully considering the end-group stoichiometry that is critical to achieve appreciable molar mass in condensation reactions. Different procedures were followed, exploring the best conditions that provided the most consistent products (see Supporting Information for details). All polymerizations were performed in melt conditions (> 220 °C). Procedure A was conducted in two stages, whereby the reaction mixture was first heated to 220 °C to promote transesterification oligomerization (4 h), followed by an increase in temperature (270 °C) and a reduced pressure (≈ 50 mTorr). Procedure B was identical except that the catalyst concentration was doubled with respect to Procedure A. In both of these procedures, it was observed that DMT sublimated and collected on the cooler rim of the reactor/flask. The stoichiometry of the feed was thus compromised, and proved problematic. In an effort to circumvent this issue, Procedure C was developed wherein a small quantity (~ 1 mL) of toluene was added to the reaction mixture and the first transesterification stage was prolonged to 16 h. This procedure caused continuous reflux of the toluene, effectively washing the sublimated DMT back into the reaction mixture. The catalyst employed in this work is based on an industrially common transesterification catalyst, tetrabutyl titanate ($Ti(OBu)_4$; TBT). This is commonly used for high temperature (> 200 °C) melt polycondensations to produce commodity polyesters such as PBT. We employed relatively high concentrations of TBT (400 or 750 ppm; see Supporting Information) in an effort to promote reaction with the statically and electronically hindered isosorbide. While the reaction was successful, this high concentration of TBT catalyst may have an impact on the final color of the material (vide infra). Synthetic protocols were executed with a 1:1 ratio of alcohol to COOMe (see Supporting Information for recipes, Table S1). We assume that the final materials have an excess of alcohol owing to the inadvertent loss of DMT during synthesis.

Various samples were made covering a wide range of target compositions by adjusting the feed ratios (Table 1). The three different procedures were applied for different compositions, as indicated. After the prescribed reaction time, the reaction mixture was cooled to ambient temperature, dissolved in a 95:5 mixture of chloroform:hexafluoroisopropanol (HFIP), and precipitated into methanol. Compositions of isolated polymers were analyzed by ^{1}H NMR spectroscopy. Signals from the PEG and ISB were used to calculate molecular makeup (Figure 2; Figure S1). The terephthalate content was consistent with the expected distribution based on the PEG and ISB. The compositions of the respective copolymers provided in Table 1 were calculated, using the signal intensities from ^{1}H NMR spectroscopy. The molar mass was estimated by ^{1}H NMR spectroscopy by assuming (and confirming) the final structure has an excess of hydroxyl groups. This was expected based on the observation described above, wherein sublimation of DMT takes place to some extent during transesterification. The molar mass is therefore calculated by comparing the ratio of ISB and PEG segments to terephthalate units. The excess was confirmed, with the ratio of signals from ISB + PEG units being slightly greater than terephthalate units (see Eq 2 in Supporting Information).

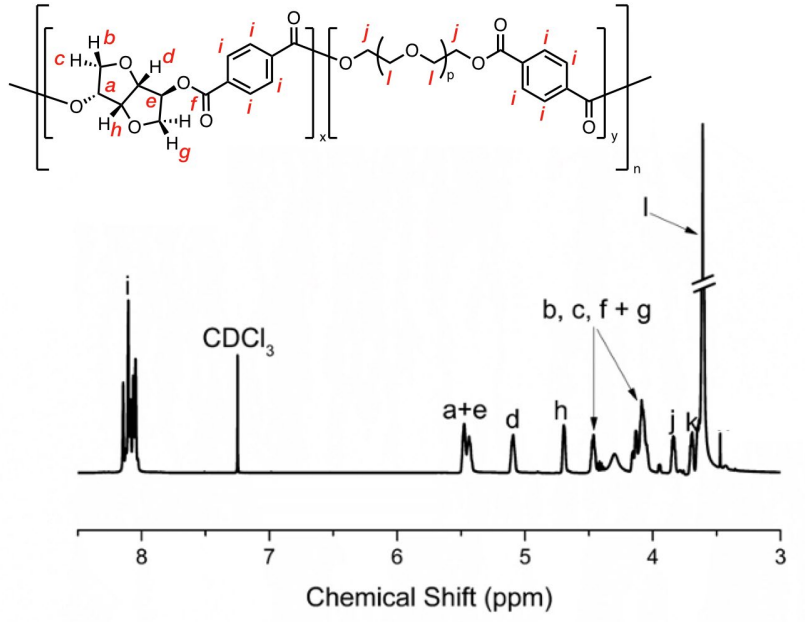

Figure 2. ^{1}H NMR spectrum of sample P4 in $CDCl_3$, with relevant signals assigned according to the displayed chemical structure.

		Target (Feed) Composition			Measured Composition								
Polymer	**Procedure[a]**	**PEG (wt %)**	**SB (wt %)[b]**	**Length HB[c]**	**PEG (wt %)**	**SB (wt %)[b]**	**Length HB[c]**	**Hard block length from ^{13}C-NMR[d]**	**$M_{n,NMR}$ (kg mol^{-1})[e]**	**$M_{n,SEC}$ (kg mol^{-1})[f]**	**Đ[g]**	**% of TP in PEG-PEG blocks**	**Yield**
P1	B	71	80	1.8	87	98	0.61	ND	ND	30.8	3.1	ND	36%
P2	B	62	70	2.7	74	84	1.44	3.41	8.1	38.3	2.0	21%	74%
P3	B	53	60	3.5	66	74	2.13	3.68	4.7	25.3	2.9	12%	61%
P4	A	50	57	4.1	63	72	2.37	4.11	8.7	34.4	2.0	11%	68%
P5	C	55	62	3.3	61	69	2.65	4.27	7.1	18.7	2.4	10%	87%
P6	C	50	57	4.1	59	67	2.85	4.47	4.7	14.5	2.7	9%	76%
P7	C	45	51	5	52	58	3.84	5.39	4.4	14.6	2.3	6%	86%
P8	C	40	45	6.1	49	55	4.32	6.16	10.2	19.7	2.1	0%	85%
P9	A	35	40	7.6	46	53	4.73	5.59	5.5	17.6	7.8	4%	75%
P10	C	35	40	7.6	39	44	6.47	7.56	5.9	10.3	4.2	5%	70%
P11	C	30	34	9.5	36	41	7.29	9.12	3.2	8.7	4.6	0%	61%
P12	A	20	23	16.4	26	30	11.5	12.3	7.3	14.9	4.4	0%	73%

(a) Refers to different procedures used, as described in detail in the Supporting Information file. (b) Soft block (SB) content calculated based on the SB repeating unit structure, which includes one PEG block and one terephthalate unit. (c) Statistical average hard block (HB) length calculated assuming a random distribution, ignoring possible differences in reactivity of the respective blocks. (d) Statistical HB length as calculated from the sequence distributions uncovered by ^{13}C NMR spectroscopic measurements (vide infra). (e) Approximate M_n calculated based on excess of alcohols with respect to therephthalate (see Supporting Information). (f) Relative M_n measured from SEC using polystyrene standards (g) Dispersities measured from SEC.

Relative segment length is an important factor next to the overall composition. Sequence or segment length has direct implications on the thermal properties and ultimately the microphase separation (i.e. average domain size). These factors subsequently link directly with mechanical properties and thus determine suitability in various applications and processing (e.g., injection molding).

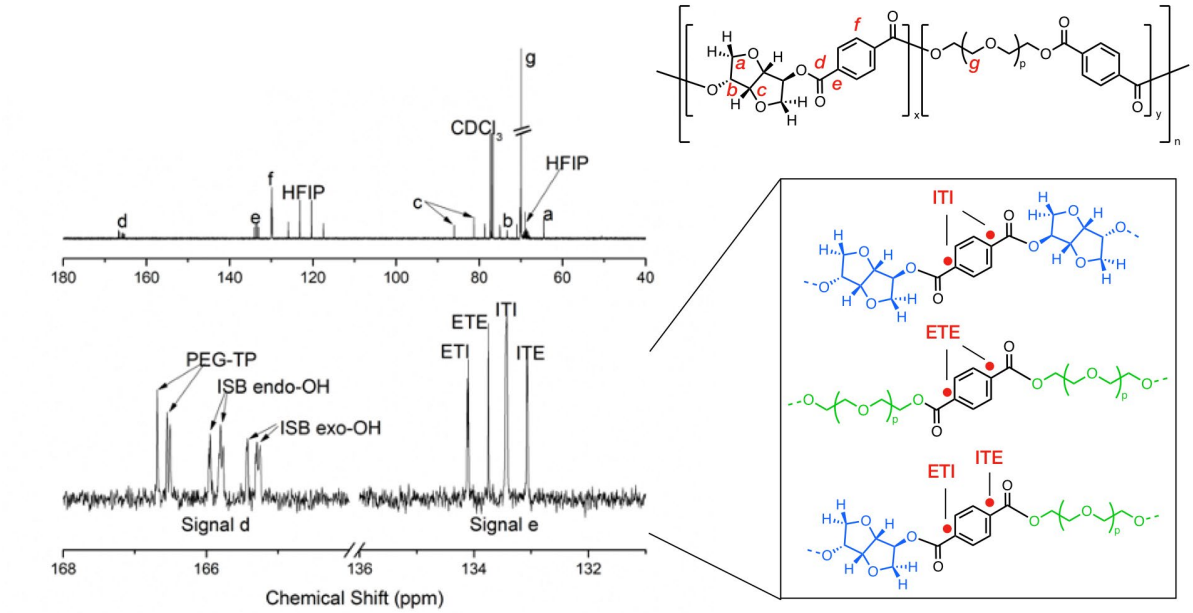

Figure 3. ^{13}C NMR spectrum of sample P4. The carbonyl region (*d*, left bottom) and quaternary aromatic region (*e*, right bottom) have been expanded. The carbonyl region shows that the ISB is incorporated randomly in blocks, rather than being endgroups. The relative integrations of the rotameric peaks are ca. 1:2, indicating that the bond is freely rotating. The quaternary aromatic shows the relative diads of ethoxy (E) and isosorbyl (I) esters on the terephthalate (T).

The ^{13}C NMR spectra enable the identification and quantification of carbons at the interface of hard block and soft block segments. This has routinely been done with copolyesters from polycondensations, particularly containing ISB-terephthalates (Figure 3; Figure S2).[28] This allows the approximate segment length to be calculated and compared to the segment lengths predicted based on completely statistical distribution (Table 1). The segment length of the hardblocks were routinely shorter than the statistical lengths predicted based on feed composition. The lower incorporation of ISB in the final polymers are consistent with this observation. The measured hard block segment lengths are in line with the calculated values when taking the actual measured composition into consideration. Procedure C provided samples with target compositions much closer to the feed ratios and calculated segment lengths reflect this (Figure 4).

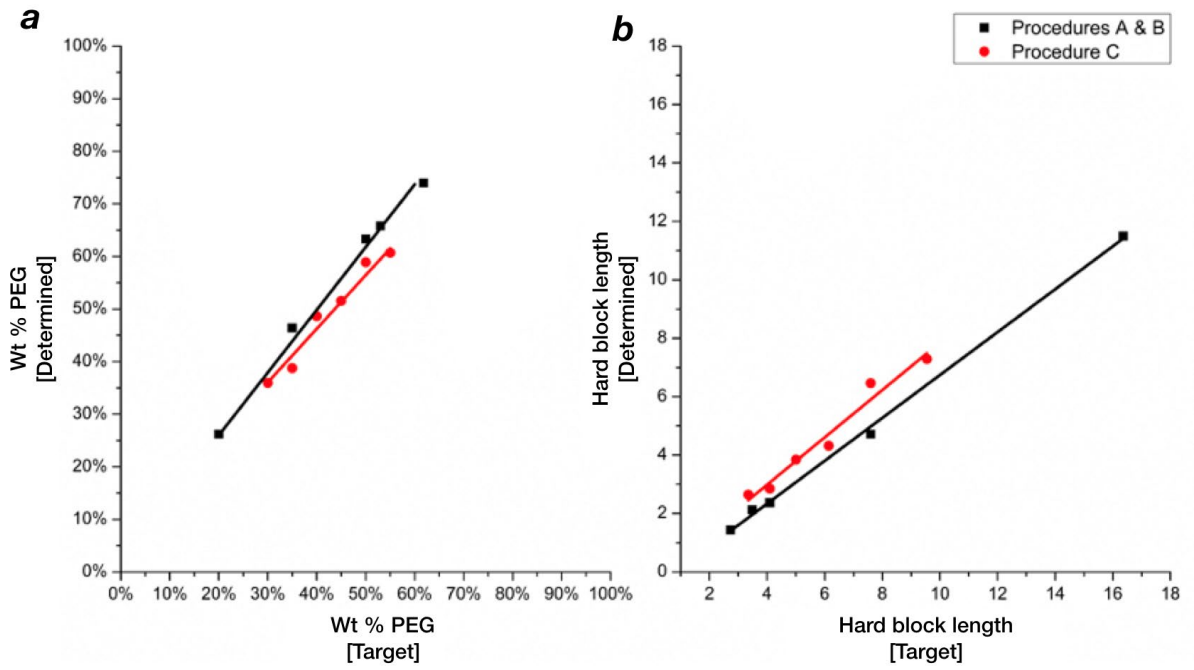

Figure 4. (a) Target compositions versus measured compositions from ^{1}H NMR spectroscopy and (b) target hard block lengths versus measured lengths from ^{13}C NMR spectroscopy, comparing the results from Procedures A, B, and C.

Relative molar masses were determined by size exclusion chromatography (SEC) with chloroform as eluent (Figure 5). All samples were readily soluble in chloroform, and provided chromatograms with dispersities (Đ) consistent with anticipated step-growth polymerizations (i.e, most probable distribution) (Table 1). All samples have moderately high molar mass, indicating some substantial conversion and suggesting that stoichiometric balance could be reasonably maintained. However, there are some notable differences. A general trend toward higher relative molar mass with increasing soft block content is observed. This may be anticipated due to the statistically larger increase in molar mass with each effective condensation reaction. In essence, the proportion of hydroxyl groups contributed from PEG is larger with higher soft block content, and each ester formed therefore has a significant impact on the molar mass. There is also a general trend of higher dispersity with lower soft block content, with sample P9 being a notable exception, with a long tail in the chromatogram toward higher molar mass. This sample therefore has a very high mass average molar mass (M_w = 137 kg mol^{-1}), relative to polystyrene standards. Although the true molar mass may be substantially lower than this, it is evident that sample P9 has a non-negligible proportion of high molar mass species, which likely influences the mechanical properties to an appreciable extent (*vide infra*). At this moment, it is unclear the origin of this clear difference in molecular makeup, and we believe it to have been a fortuitous outcome, one that is difficult to reliably reproduce.

The analysis of molar mass by complementary methods of SEC and end-group analysis are incongruous (Table 1). This may arise from the challenges with feed concentrations and targeting stoichiometric balance, in addition to the complications observed during the various synthetic protocols. Specifically, during synthesis, the formation of by-products or the loss of DMT by sublimation may have caused substantial deviation from the original target [OH]:[COOMe] ratios (e.g., elimination or etherification). The analysis of molar mass by ^{1}H NMR spectroscopy relies on the assumption that all end-groups are hydroxyl groups. Deviation from this assumption can lead to inaccurate values. While the trends in molar masses are consistent between the methods, neither value accurately reflects the true value. Nevertheless, the trends are consistent with the mechanical properties evaluated (vide infra).

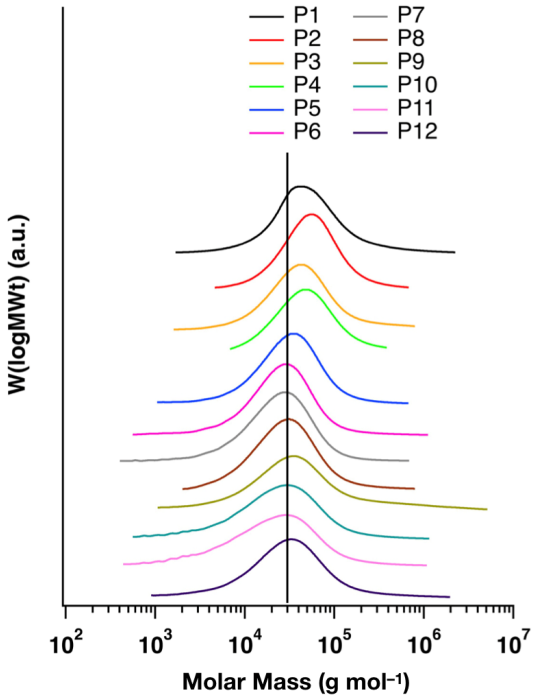

Figure 5. SEC chromatograms for polymer samples P1–P11, with chloroform as eluent and molar masses reported relative to polystyrene standards. Chromatograms have been shifted vertically and magnitudes have been normalized. A vertical line has been added for visual reference at 30 kg mol^{-1}.

The thermal characteristics of the samples was evaluated by differential scanning calorimetry (DSC). Independent of composition, it was anticipated that all samples would be completely amorphous based on previous ISB-terephthalate copolymers.[38, 41] ISB-terephthalate segments have been reported to be amorphous with a high glass transition temperature (T_g > 200 °C). The TPEE samples prepared here have thermal transitions for the

most part consistent with previous reports. However, we see in several samples a crystallization event upon heating (Figure 6a; sample P4, P6, P9). The enthalpies associated with this transition are remarkably low (See Supporting Information, Table S2). As such, we do not anticipate that they will contribute much to the mechanical properties. There is also a very broad melting event for several samples, which is so low in magnitude that it is nearly undetectable visually in Figure 6a. A magnified version of the thermograms is provided in the Supporting Information file (Figure S3). Each sample also has a relatively low T_g between –20 and –50 °C that can be attributed to the soft PEG block. The melting/crystallization transitions are difficult to confidently ascribe to the ISB-terephthalate blocks. Such segments have been routinely described as amorphous in copolymers with engineering polyesters in the past.[41, 44] Nevertheless, these transitions are of such low magnitude that the samples can be considered as nearly completely amorphous. Cooling thermograms and sample appearance as films are consistent with this conclusion (Figure 6b; *vide infra*). There is a clear exception to this trend in sample P1. P1 has such a high concentration of PEG soft block that there is a significant portion that is not tethered within a copolyester. Therefore, the thermal signature of PEG homopolymer is observed for this sample.

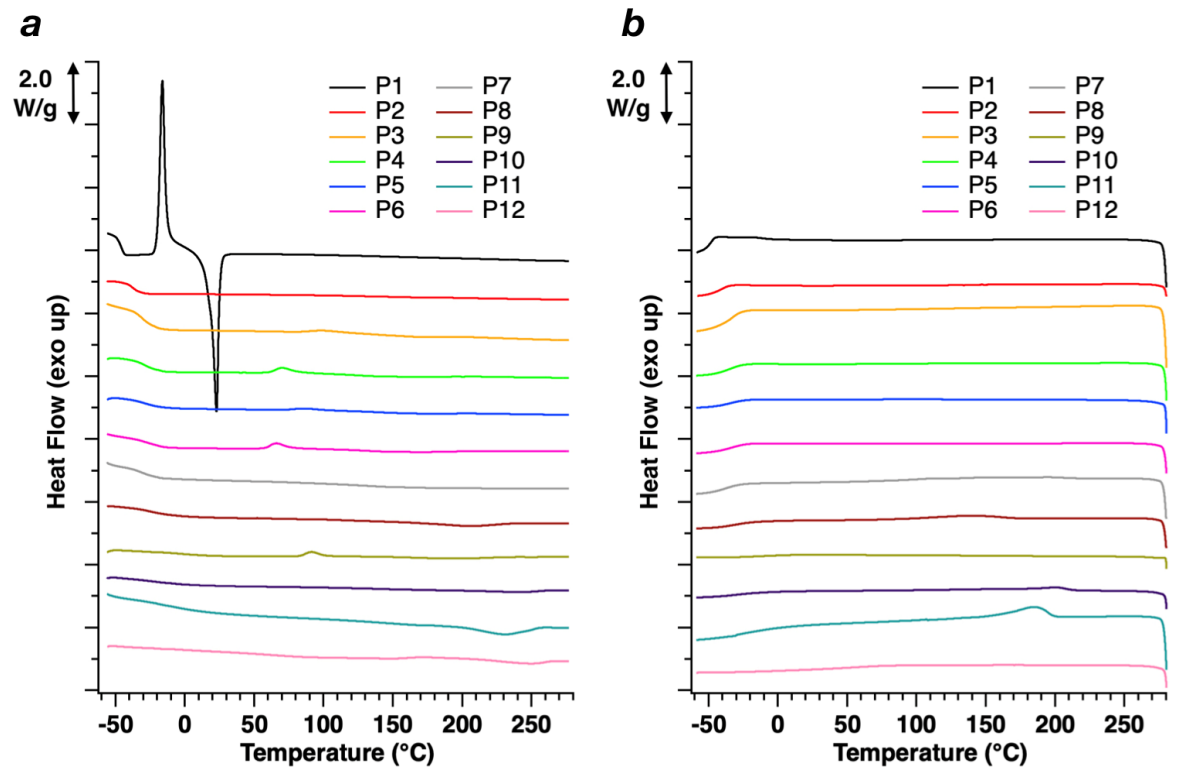

Figure 6. DSC thermograms showing (a) the second heating and (b) the cooling profiles for samples P2–P11.

Samples were melt pressed between 120 and 200 °C using a hydraulic press for ca. 5 min. The pressed films were subsequently cooled rapidly by removing from the press and clamping between metal plates at ambient temperature. The samples were cut into dogbone shapes. Each sample was transparent but darkly colored, consistent with previous observations (Figure S4).[25, 26, 48] The dog bones were subjected to uniaxial tensile testing, whereby they were extended until failure. The stress–curves were analyzed for the primary mechanical features, including elastic modulus, and stress and strain at break (Figure 7).

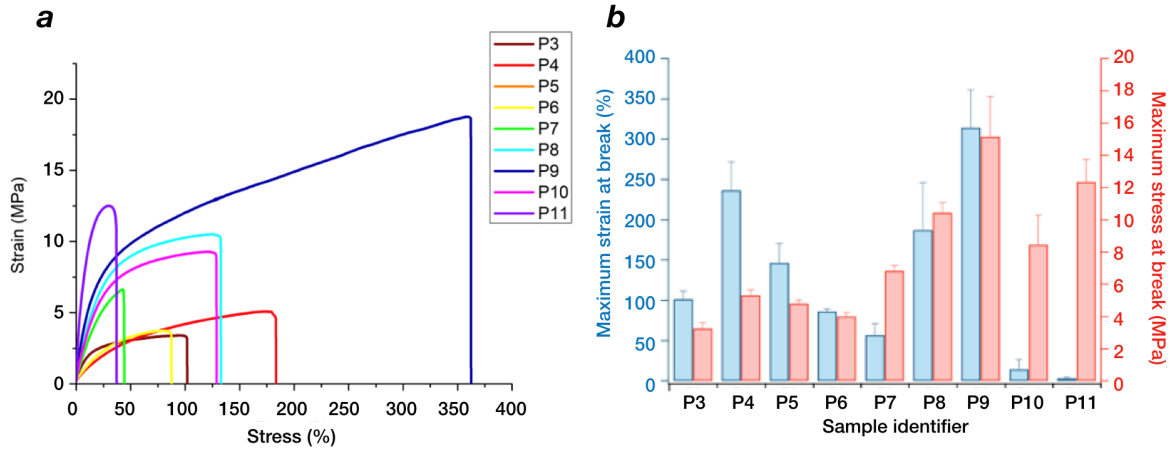

Figure 7. (a) Selected stress–strain curves for samples P3–P11 and (b) the extracted maximum stress and strain at break.

The values for the measured samples are summarized in Table 2. The general trend shows a nearly monotonic increase in elastic modulus with increasing hard block content, consistent with expectations. Clearly all the materials that were measured have relatively high elastic modulus, consistent with commercially available TPEEs in a comparable composition range. However, the strain at break was consistently lower than 200%, with one exception (P9), suggesting that the molar masses are not adequately high enough. While the number-average molar masses are rather spread from sample to sample, the weight average molar mass of sample P9 is the largest by a significant margin, owing to the high molar mass tail shown in the SEC chromatogram and the correspondingly large dispersity (P9, Đ = 7.8; M_w = 137 kg mol^{-1}). The mechanical properties are thus in line with the SEC measurements, the low reactivity of the ISB monomer, and the challenge associated with stoichiometric balance. However, it is clear that Procedure C provided the highest molar mass and consequently the materials with the most impressive mechanical properties. In all cases, however, much higher molar mass could foreseeably be achieved with a process that is more akin to commercial TPEE production (e.g., mechanical stirring). This presents opportunities to improve in future endeavors, but nevertheless indicates a promising approach to making mechanically robust TPEEs with the renewable ISB as a component.

Table 2. Mechanical characteristics extracted from the tensile tests.

Material	Elastic Modulus (MPa)	Max Stress (MPa)	Strain at Break (%)
P1	ND	ND	ND
P2	ND	ND	ND
P3	1.23 ± 0.80	3.27 ± 0.36	101.8 ± 10.1
P4	1.17 ± 0.34	5.33 ± 0.32	237.2 ± 35.4
P5	2.21 ± 0.45	4.81 ± 0.23	146.9 ± 23.7
P6	1.53 ± 0.45	4.02 ± 0.22	86.6 ± 2.6
P7	2.86 ± 0.36	6.84 ± 0.31	57.3 ± 13.8
P8	4.55 ± 0.48	10.46 ± 0.65	187.6 ± 58.7
P9	6.58 ± 0.84	15.19 ± 2.45	315.0 ± 46.9
P10	24.32 ± 0.82	8.47 ± 1.85	14.6 ± 12.0
P11	66.51 ± 2.42	12.36 ± 1.39	3.7 ± 1.11
P12	ND	ND	ND

CONCLUSION

A series of TPEEs with a partially biobased hard block and a PEG soft block was prepared using bulk melt polycondensation. A range of compositions was explored, with mechanical properties consistent with the soft block to hard block ratio. Owing to challenging circumstances related to achieving the stoichiometric balance that is critical for obtaining high conversions, predominantly low molar masses were obtained. Nevertheless, several reaction conditions were investigated that provided some promising materials exhibiting impressive tensile properties. This serves as a promising stepping stone, indicating that commercially relevant materials can potentially be accessed by further fine tuning of the reactor setup. We are actively exploring the propensity of isosorbide as a sustainable alternative resource for making TPEEs with a range of co(macro)monomers. A custom-built melt reactor with high torque capabilities to promote further reaction would be essential for pushing these reactions beyond the current limit encountered in this work. As such, we are keen to explore such alternatives within this promising arena.

ACKNOWLEDGMENTS

We gratefully acknowledge the support of the Flemish Government and Flanders Innovation & Entrepeneurship (VLAIO) through the Moonshot project CoRe^2 (HBC2019.0116). This work is further supported by Hasselt University and the Research Foundation Flanders (FWO Vlaanderen) via the Hercules project AUHL/15/2 - GOH3816N.

ORCID

Bryn Monnery: https://orcid.org/0000-0001-5691-5451

Apostolos Karanastasis: https://orcid.org/0000-0001-9966-7873

Peter Adriaensens: https://orcid.org/0000-0003-4183-0150

Louis M. Pitet: https://orcid.org/0000-0002-4733-0707

SUPPORTING INFORMATION

Additional supporting information may be found online in the Supporting Information section at the end of this article.

REFERENCES

[1] G. J. E. Biemond, J. Feijen, R. J. Gaymans, *Polym. Eng. Sci.* **2008**, *48*, 1389-1400.
[2] R. J. Cella, *J. Polym. Sci.: Polym. Symp.* **1973**, *42*, 727-740.
[3] W. Gabrielse, M. Soliman, K. Dijkstra, *Macromolecules* **2001**, *34*, 1685-1693.
[4] T. H. Hao, C. Zhang, G. H. Hu, T. Jiang, Q. C. Zhang, *J. Appl. Polym. Sci.* **2016**, *133*.
[5] R. K. Adams, G. K. Hoeschele, W. K. Witsiepe, in *Thermoplastic Elastomers*, 3rd ed. (Eds.: G. Holden, H. R. Kricheldorf, R. P. Quirk), Hanser, **2004**, pp. 183–216.
[6] X. G. Li, G. Song, M. R. Huang, Y. B. Xie, *ACS Sustainable Chem. Eng.* **2018**, *6*, 9074-9085.
[7] R. J. Gaymans, *Prog. Polym. Sci.* **2011**, *36*, 713-748.
[8] Y. Q. Zhu, C. Romain, C. K. Williams, *Nature* **2016**, *540*, 354-362.
[9] D. K. Schneiderman, M. A. Hillmyer, *Macromolecules* **2017**, *50*, 3733-3750.
[10] D. E. Fagnani, J. L. Tami, G. Copley, M. N. Clemons, Y. D. Y. L. Getzler, A. J. McNeil, *ACS Macro Lett.* **2021**, *10*, 41-53.
[11] G.-Q. Chen, M. K. Patel, *Chem. Rev.* **2012**, *112*, 2082-2099.
[12] A. Gandini, T. M. Lacerda, *Prog. Polym. Sci.* **2015**, *48*, 1-39.
[13] B. A. J. Noordover, A. Heise, P. Malanowski, D. Senatore, M. Mak, L. Molhoek, R. Duchateau, C. E. Koning, R. A. T. M. van Benthem, *Prog. Org. Coat.* **2009**, *65*, 187-196.
[14] J. A. Galbis, M. de Gracia Garcia-Martin, M. Violante de Paz, E. Galbis, *Chem. Rev.* **2016**, *116*, 1600-1636.
[15] C. Vilela, A. F. Sousa, A. C. Fonseca, A. C. Serra, J. F. J. Coelho, C. S. R. Freire, A. J. D. Silvestre, *Polym. Chem.* **2014**, *5*, 3119-3141.
[16] R. Storbeck, M. Rehahn, M. Ballauff, *Makromolekulare Chemie-Macromolecular Chemistry and Physics* **1993**, *194*, 53-64.
[17] H. R. Kricheldorf, *J. Macromol. Sci., Rev. Macromol. Chem. Phys.* **1997**, *C37*, 599-631.
[18] S. Munoz-Guerra, C. Lavilla, C. Japu, A. M. de Ilarduya, *Green Chem.* **2014**, *16*, 1716-1739.
[19] C. Lavilla, A. M. de Ilarduya, A. Alla, M. G. Garcia-Martin, J. A. Galbis, S. Munoz-Guerra, *Macromolecules* **2012**, *45*, 8257-8266.

[20] C. Lavilla, A. Alla, A. M. de Ilarduya, S. Munoz-Guerra, *Biomacromolecules* **2013**, *14*, 781-793.
[21] C. Lavilla, A. M. de Ilarduya, A. Alla, S. Munoz-Guerra, *Polym. Chem.* **2013**, *4*, 282-289.
[22] C. Lavilla, E. Gubbels, A. M. de Ilarduya, B. A. J. Noordover, C. E. Koning, S. Munoz-Guerra, *Macromolecules* **2013**, *46*, 4335-4345.
[23] J. C. Morales-Huerta, A. M. de Ilarduya, S. Leon, S. Munoz-Guerra, *Macromolecules* **2018**, *51*, 3340-3350.
[24] L. Jasinska, C. E. Koning, *J. Polym. Sci., Part A: Polym. Chem.* **2010**, *48*, 5907-5915.
[25] R. Quintana, A. M. de Ilarduya, A. Alla, S. Munoz-Guerra, *J. Polym. Sci., Part A: Polym. Chem.* **2011**, *49*, 2252-2260.
[26] C. Gioia, M. Vannini, P. Marchese, A. Minesso, R. Cavalieri, M. Colonna, A. Celli, *Green Chem.* **2014**, *16*, 1807-1815.
[27] Y. Chebbi, N. Kasmi, M. Majdoub, P. Cerruti, G. Scarinzi, M. Malinconico, G. Dal Poggetto, G. Z. Papageorgiou, D. N. Bikiaris, *ACS Sustainable Chem. Eng.* **2019**, *7*, 5501-5514.
[28] C. Lavilla, S. Munoz-Guerra, *Green Chem.* **2013**, *15*, 144-151.
[29] J. Wu, P. Eduard, S. Thiyagarajan, L. Jasinska-Walc, A. Rozanski, C. F. Guerra, B. A. J. Noordover, J. van Haveren, D. S. van Es, C. E. Koning, *Macromolecules* **2012**, *45*, 5069-5080.
[30] J. Wu, P. Eduard, L. Jasinska-Walc, A. Rozanski, B. A. J. Noordover, D. S. van Es, C. E. Koning, *Macromolecules* **2013**, *46*, 384-394.
[31] J. Wu, P. Eduard, S. Thiyagarajan, B. A. J. Noordover, D. S. van Es, C. E. Koning, *Chemsuschem* **2015**, *8*, 67-72.
[32] L. Gustini, C. Lavilla, A. M. de Ilarduya, S. Munoz-Guerra, C. E. Koning, *Biomacromolecules* **2016**, *17*, 3404-3416.
[33] C. Lavilla, A. Alla, A. M. de Ilarduya, E. Benito, M. G. Garcia-Martin, J. A. Galbis, S. Munoz-Guerra, *Biomacromolecules* **2011**, *12*, 2642-2652.
[34] C. Lavilla, A. Alla, A. M. de Ilarduya, E. Benito, M. G. Garcia-Martin, J. A. Galbis, S. Munoz-Guerra, *J. Polym. Sci., Part A: Polym. Chem.* **2012**, *50*, 3393-3406.
[35] C. Lavilla, E. Gubbels, A. Alla, A. M. de Ilarduya, B. A. J. Noordover, C. E. Koning, S. Munoz-Guerra, *Green Chem.* **2014**, *16*, 1789-1798.
[36] O. Kreye, S. Oelmann, M. A. R. Meier, *Macromol. Chem. Phys.* **2013**, *214*, 1452-1464.
[37] A. Alla, K. Hakkou, F. Zamora, A. M. de Ilarduya, J. A. Galbis, S. Munoz-Guerra, *Macromolecules* **2006**, *39*, 1410-1416.
[38] J. Y. Chen, J. Wu, J. F. Qi, H. P. Wang, *ACS Sustainable Chem. Eng.* **2019**, *7*, 1061-+.
[39] H. R. Kricheldorf, S. M. Weidner, *Macromol. Chem. Phys.* **2013**, *214*, 726-733.
[40] M. Majdoub, A. Loupy, G. Fleche, *Eur. Polym. J.* **1994**, *30*, 1431-1437.
[41] H. R. Kricheldorf, G. Behnken, M. Sell, *J. Macromol. Sci., Part A: Pure Appl. Chem.* **2007**, *44*, 679-684.
[42] C.-H. Lee, H. Takagi, H. Okamoto, M. Kato, *J. Appl. Polym. Sci.* **2013**, *127*, 530-534.
[43] N. Kasmi, N. M. Ainali, E. Agapiou, L. Papadopoulos, G. Z. Papageorgiou, D. N. Bikiaris, *Polym. Degrad. Stab.* **2019**, *169*.
[44] M. Garaleh, T. Yashiro, H. R. Kricheldorf, P. Simon, S. Chatti, *Macromol. Chem. Phys.* **2010**, *211*, 1206-1214.
[45] J. C. Bersot, N. Jacquel, R. Saint-Loup, P. Fuertes, A. Rousseau, J. P. Pascault, R. Spitz, F. Fenouillot, V. Monteil, *Macromol. Chem. Phys.* **2011**, *212*, 2114-2120.
[46] B. A. J. Noordover, V. G. van Staalduinen, R. Duchateau, C. E. Koning, R. van Benthem, M. Mak, A. Heise, A. E. Frissen, J. van Haveren, *Biomacromolecules* **2006**, *7*, 3406-3416.
[47] I. S. Ristic, N. Vukic, S. Cakic, V. Simendic, O. Ristic, J. Budinski-Simendic, *J. Polym. Environ.* **2012**, *20*, 519-527.
[48] F. Fenouillot, A. Rousseau, G. Colomines, R. Saint-Loup, J. P. Pascault, *Prog. Polym. Sci.* **2010**, *35*, 578-622.